RSC Advances

ROYAL SOCIETY OF CHEMISTRY

www.rsc.org/advances

CdS quantum dots immobilized on calcium alginate microbeads for rapid and selective detection of Hg^{2+} ions

Ambika Kumar and Raj Kumar Dutta*

Department of Chemistry, Indian Institute of Technology Roorkee, Roorkee – 247667, India

*Corresponding author: Fax: +91-1332-286202, Tel. +91-1332-285280,

Email: duttafcy@iitr.ernet.in

GRAPHICAL ABSTRACT

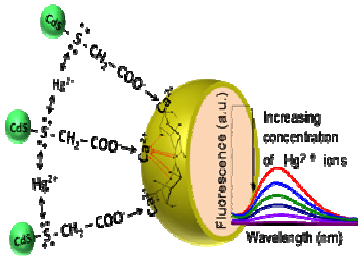

Immobilized CdS QDs for selective detection and pre-concentration of Hg^{2+}

CdS quantum dots immobilized on calcium alginate microbeads for rapid and selective detection of Hg^{2+} ions

Ambika Kumar and Raj Kumar Dutta*

Department of Chemistry, Indian Institute of Technology Roorkee, Roorkee – 247667, India

Abstract

Mercury is extremely toxic to environment and is detrimental to human health. We describe here development of an analytical method comprising mercaptoacetic acid capped CdS quantum dots (QDs) immobilized on calcium alginate microbeads (referred here as CA@CdS) for rapid, selective and quantitative detection of Hg^{2+} ions based on fluorescence quenching phenomenon. The feasibility of detecting Hg^{2+} ions in this method is extended to real time analysis by spiking 0.5 mg/L and 1.0 mg/L Hg^{2+} ions in batches of municipality tap water. The mechanism of fluorescence quenching has been explained on the basis adsorption of Hg^{2+} (adsorption capacity was determined to be 88.33 µg/g). The selectivity of Hg^{2+} ions is attributable to its soft acid-soft base interaction between Hg^{2+} and the sulphydryl group of the mercaptoacetic acid capped CdS QDs. The fluorescence quenching phenomenon satisfied Stern-Volmer equation and was linearly correlated with Hg^{2+} ions concentrations in the range of 0.015 and 2.0 mg L^{-1}. The limit of detection of Hg^{2+} ion was determined to be 0.008 mg L^{-1} at an optimized condition, i.e., pH 6 and contact time 30 min; and the detection was not affected by other experimentally relevant cations like Na^{+}, Mg^{2+}, K^{+}, Ca^{2+}, Mn^{2+}, Fe^{2+}, Cu^{2+}, Pb^{2+}, Cr^{3+}, Zn^{2+}, As^{3+}, Cd^{2+}; and anions like Cl^{-}, CO_3^{2-}, HCO_3^{-}, HPO_4^{-}, SeO_4^{-}, SO_4^{2-}. The major advantage of this nano-fluoroprobe is that it can detect as well as remove Hg^{2+} ions from aqueous medium. The fluoroprobe can be recovered and re-used for subsequent cycles of detection and removal of Hg^{2+} ions.

Keywords: Hg^{2+} detection, CdS quantum dots, fluorescence quenching, Hg^{2+} adsorption

*** Corresponding Author**. Email: duttafcy@iitr.ac.in; Tel: +91 1332 285280

1. Introduction

There is a growing demand for developing efficient sensors for detection of mercury ions (Hg^{2+}) in the environment,[1-4] owing to its toxicity to ecosystem and its adverse effect on health.[5-7] Mercury contamination is primarily attributable to anthropogenic source where it is released from various types of industries into air and water.[8,9] The safe limit of mercury in drinking water in any chemical form is set as 0.002 mg L^{-1} by US Environmental Protection Agency (EPA).[10] This demands rapid, economical and selective detection of mercury at a concentration comparable to environmental levels. Determination of mercury at such low concentration in presence of other cations and anions by conventional instrumental techniques like cold vapor atomic absorption spectrometry (CV-AAS),[11] ICP-MS hyphenated with gas chromatograph (GC-ICP-MS)[12] and atomic fluorescence spectrometry coupled with reversed phase high performance liquid chromatography,[13] has posed a analytical challenges associated with time consuming sample preparation and pre-concentration steps. This has urged the importance of developing alternate methodologies for fast detection of mercury ions of concentration significant to environmental concentrations. It is worthwhile to mention about the two comprehensive and systematic review work illustrating wide range of methodologies on mercury ion sensors published by Lippard's group (in 2008)[14] and recently by Chen's group (in 2015).[15]

The large number of colorimetric methods that has been developed are based on chemical bonding between specifically designed molecules with Hg^{2+} ions and resulted in sharp changes in the colour. This concept has been well executed to make optical strips and chemidosimeters suitable for field analysis of Hg^{2+} ions.[16-19] Nanomaterials are also reported as excellent Hg^{2+} ion sensor owing to excellent optical property and stability. Notably, fast mercury ion detection has been reported using functionalized gold nanoparticles.[20-23] Besides, quantum dot (QD) based fluoroprobes made of ZnS, ZnSe, CdSe and CdTe are also reported as excellent probes for

mercury ion detection based on fluorescence quenching.[24-27] Though CdS QDs exhibit excellent fluorescence emission property but so far its application as Hg^{2+} sensor has been limited.[28]

One of the major limitations of using semiconductor type quantum dots as Hg^{2+} ion sensor is attributable to its dispersion due to a tendency of agglomeration in the analyte which would likely to affect the measurement of optical property. We present here a simplistic approach for developing a nano-fluoroprobe where CdS quantum dots were immobilized on calcium alginate microbeads where on one hand the fluorescence property of CdS QDs is not compromised and on the other hand the intricacies of optical measurement of an analyte interfered by dispersion of nanoparticles is avoided. The choice of CdS QDs is pertinent as it is expected to exhibit fluorescence quenching on interaction with Hg^{2+} ions.[29] The calcium alginate was chosen as a substrate for anchoring CdS QDs as calcium alginate microbeads did not interfere on the fluorescence property of CdS QDs. The fluoroprobe developed for this study is referred to as calcium alginate coated with CdS QDs and will be henceforth represented as CA@CdS microbeads. Apart from Hg^{2+} ion detection at $\mu g.L^{-1}$ (i.e., parts per billion) concentration the synergistic removal of adsorbed Hg^{2+} ion from aqueous medium by gravity was an added advantage.

2. Experimental

2.1. Chemicals

Sodium alginate powder, calcium chloride (98%, w/v), cadmium chloride (98%, w/v), mercaptoacetic acid (80%, v/v), sodium sulphide (58-62%, w/v), mercuric chloride (99.5%, w/v), toluene (99%, v/v), sodium hydroxide (98%, w/v), nitric acid (70%), hydrochloric acid (35%, v/v), ethylenediaminetetraacetic acid (EDTA) di-sodium salt and acetone were procured from Himedia Pvt. Ltd. India. The sodium salts of acetate, borohydride, chloride, carbonate, bicarbonate, hydrogen phosphate, hydroxide, selenate and sulphate used in this study were

procured from Merck India. The commercial ICP-MS standard solution of metal ions, e.g., Na^{+}, Mg^{2+}, K^{+}, Ca^{2+}, Hg^{2+}, Cu^{2+}, Pb^{2+}, As^{3+}, Cd^{2+}, Fe^{2+}, Co^{2+}, Cr^{3+}, Zn^{2+}, Mn^{2+} were purchased from Merck, India. All chemicals used in this study were not subjected to any further purification.

2.2. Synthesis and characterization of CA@CdS microbeads

The fabrication of CA@CdS microbeads comprised of two steps, e.g., (a) synthesis of water soluble CdS quantum dots (CdS QDs) by chemical precipitation method and stabilized by mercaptoacetic acid;[30] (b) synthesis of calcium alginate microbeads *in situ* coated with as-synthesized CdS QDs. The optimized result was obtained when 1.5 g of sodium alginate powder was mixed with 100 mL of freshly prepared CdS QDs and homogenized by constant magnetic stirring for 3 h. This mixture was added drop-wise into $CaCl_2$ solution (2.0% w/v) through a micro-tip nozzle and stirred for 6 h to form spherical shaped calcium alginate microbeads coated with CdS QDs, which will henceforth be referred to as CA@CdS microbeads. These microbeads were then kept at 4 ^{o}C for 24 h to impart rigidity. These microbeads were washed several times with deionised water to remove impurities and then oven dried at 50 ^{o}C for overnight. The concentration of CdS in the batches of CA@CdS synthesized was determined to be 14.32 % w/w.

2.3. Characterization techniques

The X-ray powder diffraction (XRD) patterns were recorded on Bruker ARS D8 Advance diffractometer using graphite monochromatized Cu K_{α} radiation (λ =1.5406 Å) in a 2θ range from 20^{o} to 80^{o} at a scanning rate of 2^{o}/min. Field emission scanning electron microscopy (FESEM) images were recorded with Zeiss Ultra plus based ultra 55, operating at an accelerating voltage of 20 kV. The elemental composition of the nanoparticles was determined by energy dispersive X-ray spectrometer (EDX) attached with the FESEM. Transmission electron

microscopy (TEM) images were recorded with FEI Technai-G^2 microscope, operated at an acceleration voltage of 200 kV. The Fourier transformed infrared spectroscopy (FT-IR) studies were performed on Thermo NICOLET 6700 FTIR. Representative CA@CdS microbeads were powdered and pelletized with KBr. Similarly, mercaptoacetic acid was drop casted on KBr pellet. The Brunauer Emmett and Teller (BET) specific surface area of the CdS nanoparticles were measured by Quantachrome Nova 2200 analyser at liquid nitrogen temperature using nitrogen adsorption–desorption method. The UV-visible absorption spectroscopy studies of CdS QDs were recorded in the wavelength range of 200–800 nm using Shimadzu, UV-1800. The fluorescence emission spectra of CdS QDs and CA@CdS microbeads were recorded using HORIBA FluorEssence Spectrometer (FluoroMax-4) at an excitation wavelength (λ_{ex}) of 375 nm.

2.4. Fluorescence quenching studies

The UV-visible absorption spectrum of the as-synthesized CdS QDs revealed maximum absorbance at 343 nm, corresponding to a large band gap of 3.2 eV (Fig. 1a) and our result was comparable with the reported literature.[31] The fluorescence emission spectrum recorded at excitation wavelength of 375 nm revealed a broad and strong peak at 534 nm (Fig. 1b), which was similar to that reported in literature.[32] The pH and the contact time for fluorescence quenching were optimized by treating the batches of CA@CdS microbeads with 1 mg L^{-1} Hg^{2+} ion solution. The maximum fluorescence quenching was recorded at pH = 6, (Fig. 2). The optimum contact time was determined from a kinetic study at pH 6, by measuring the fluorescence intensity of the microbeads treated with Hg^{2+} solution (1 mg L^{-1}) at selected time intervals. The fluorescence intensity decreased with contact time and a saturation condition was obtained after 30 min (Fig. 3). The saturation time determined in our method was lesser as compared to most of the methods that are cited in a recent review work by Chansuvarn et al.[33]

Systematic fluorescence quenching studies were performed by treating batches of 0.375 g of CA@CdS microbeads with 50 mL of Hg^{2+} ions in the concentration range between 0.1 mg L^{-1} (100 parts per billion) and 200 mg L^{-1} (200 parts per million) at optimum condition, i.e., pH 6 and contact time of 30 min. Detection of Hg^{2+} ion concentrations less than 100 μg/L was performed using 250 mL and 1250 mL of Hg^{2+} ion solution. In this study a standard Hg^{2+} ion solution of 1000 mg L^{-1} (Merck, India) was used and all the required batches of Hg^{2+} ion concentrations were prepared by serial dilution in de-ionized water (Millipore, Ω = 18 mega Ohm).

2.5. Selectivity and interference measurement

The selectivity of CA@CdS microbeads towards Hg^{2+} ions detection was investigated by treating microbeads with the batches of 10 mg L^{-1} of the cations, *viz*, Na^{+}, K^{+}, Mg^{2+}, Ca^{2+} Cd^{2+}, Cr^{3+}, Fe^{2+}, As^{3+}, Mn^{2+}, Pb^{2+}, Cu^{2+}, Zn^{2+} and Hg^{2+}, respectively at the optimized conditions. The solutions of the above metal ions were prepared from their respective elemental standard solutions (1000 mg L^{-1}, Merck India) after serial dilution in deionised water (Millipore). The possible anion interferences in the Hg^{2+} ion detection was studied by treating 1mM anions of respective sodium salts (Merck, India), e.g CH_3COO^-, Cl^-, CO_3^{2-}, HCO_3^-, HPO_4^-, OH^-, SeO_4^- SO_4^{2-} and BH_4^- at optimized conditions.

2.6. Quantitative estimation of Hg^{2+} adsorbed on CA@CdS microbeads by ICP-MS

A batch of 250 mL (i.e., 5 x 50 mL) of 1 mg L^{-1} Hg^{2+} ion solution was treated with 1.875 g (i.e., 5 x 0.375 g) CA@CdS microbeads at pH 6. Aliquot of about 4 mL of the supernatant solution were removed at selected time intervals ranging between 5 min and 90 min contact time and the Hg^{2+} ion concentration in each batch was estimated by ICP-MS (Perkin Elmer Sciex, equipped with ELAN DRC-e facility) after suitable calibration. The concentration of Hg^{2+} ions adsorbed

on CA@CdS microbeads was calculated from the difference between original Hg^{2+} concentration taken (i.e., 1 mg L^{-1}) and the concentration measured by ICP-MS.

3.0. Results and Discussion

3.1. Characterization of CdS quantum dots (QDs)

The XRD pattern of the as synthesized CdS QDs exhibited Bragg reflection at (111), (220) and (311) planes (Fig. 4), which was similar to the reported literature.[34] This confirmed the synthesis of cubic phase of CdS (JCPDS No. 10-454). From Debye-Scherrer equation,[35] the average crystallite size of the CdS QDs was determined as 2.54 nm. The particle size of CdS QDs measured by TEM mostly ranged between 2.0 and 4.0 nm, and the average particle size deduced from the histogram distribution was 2.77 nm (Fig. 5a). Moreover the nanocrystalline nature of the as-synthesized CdS quantum dots was reflected from observation of the lattice fringes (as marked in Fig. 5b) separated by 0.341 nm, which agreed well with atomic layer spacings reported in CdS nanocrystal.[36] The polycrystalline nature of CdS QDs was also reflected from the selected area electron diffraction (SAED) measurements (inset of Fig 5b).

The particle size measured by TEM was further confirmed from the theoretical calculation using effective mass approximation theory, given as follows:[37]

$$\Delta E_g = E_{g\ (QDs)} - E_{g\ (bulk)} = (h^2/8\mu r^2) - 1.8e^2/4\pi\varepsilon_o\varepsilon_r r$$

where, $1/\mu = 1/m_e^* + 1/m_h^*$; μ is the reduced mass of electron – hole effective mass; $m_e^* = 0.19\ m_o$ and $m_h^* = 0.80\ m_o$ (m_o is the absolute mass of electron); $\varepsilon_r = 5.7$ is the permittivity of the sample[38]. The band gap of as-synthesized CdS QDs was measured as $E_{g\ (QDs)} = 3.2$ eV (Fig.1), while the band gap for bulk CdS, $E_{g\ (bulk)} = 2.25$ eV.[39] The average particle size (2r) determined from effective mass approximation theory was 2.77 nm, which was in good agreement with the TEM measurements. The sizes of the as-synthesized CdS QDs were less than the Bohr radius of

electron and hole pair and consequently exhibited intense fluorescence emission due to quantum confinement effect.[32,40]

3.2. Characterization of CA@CdS microbeads

The FE-SEM revealed formation of spherical shaped CA@CdS microbeads of about 500 μm diameter (Fig. 6a). Higher resolution FE-SEM images revealed details of structural features at surface of the microbeads (Fig. 6b and 6c) and the EDX analysis reflected surface composition comprising of Cd and S (Fig. 6d). Further, CdS quantum dots were mostly present at the outer surface of the microbeads as confirmed from the line scan measured across the inner and outer surface of a representative CA@CdS microbead (Fig. 6e).

The results of FT-IR studies given in Fig. 7 confirmed stabilization of CdS QDs by thiol group of mercaptoacetic acid (MAA). The characteristic IR band at 2560 cm^{-1} (corresponding to S-H bond) was observed in the FT-IR spectrum of MAA while this band was absent in the spectrum of CA@CdS microbeads. This is attributable to formation of a sulphydryl group, i.e., CdS-S bond. Further, the band at 1719 cm^{-1} and shoulder peak at 1625 cm^{-1} recorded in the FT-IR spectrum of MAA corresponded to the carboxylic acid group. These signature peaks of –COOH group were absent in CA@CdS microbeads, while a new peak was observed at 1607 cm^{-1}. This is attributable to carboxylate group which is contributed from calium alginate and also by mercaptoacetic acid. The other peaks recorded at 1421 cm^{-1} corresponded to the $–CH_2$ group and those at 1086 cm^{-1} and 1032 cm^{-1} corresponded to the ether linkage in alginate. Using these data a tentative model is presented to show the anchoring of MAA capped CdS quantum dots anchored to calcium alginate microbeads via electrostatic interaction between Ca^{2+} ions in calcium alginate and the $–COO^-$ group in de-protonated MAA (Scheme 1).

3.3. Hg^{2+} ion Sensing

The CA@CdS microbeads treated with Hg^{2+} ions revealed decrease in the fluorescence intensity with increase in the Hg^{2+} ion concentrations and complete quenching was observed for the batch treated with 200 mg L^{-1} of Hg^{2+} ions (Fig 8a). The fluorescence quenching of CA@CdS microbeads treated with Hg^{2+} ion concentrations was studied using Stern-Volmer equation given as:[41]

$$I_o/I = 1 + K_{sv}[Hg^{2+}]$$

where, I_o is the fluorescence intensity of untreated CA@CdS microbeads; I is the fluorescence intensity of CA@CdS microbeads treated with Hg^{2+} ions; K_{sv} is the Stern-Volmer fluorescence quenching constant, $[Hg^{2+}]$ is the concentration of Hg^{2+} ions. The Stern-Volmer plot of I_o/I versus $[Hg^{2+}]$ was not linear over the entire concentration range of 0.1 mg L^{-1} to 200 mg L^{-1} Hg^{2+} ions. At a lower concentration of Hg^{2+} ion, i.e., 0.1 mg L^{-1} and 2.0 mg L^{-1}, the plot was linear (R^2 = 0.98, Fig 7b), which is attributable to dynamic range for quantitative estimation of Hg^{2+} ions by fluorescent quenching technique. The K_{sv} value (0.682 L/mg) was determined from the slope of the linear plot.

The limit of detection (LOD) of Hg^{2+} ions was calculated as 8.16 µg L^{-1} using the expression 3σ/*s*, where 'σ' is the standard deviation of the fluorescence intensity of the CA@CdS microbeads not treated with of Hg^{2+} ions. Similarly the limit of quantification (LOQ) was calculated to be 27.18 µg L^{-1}, using the expression 10σ/*s*. The value of *'s'* was obtained from the slope of the fluorescence emission intensity of the CA@CdS microbeads treated with Hg^{2+} ion concentrations in the range of 0.1 and 2.0 mg L^{-1}, as shown in Fig. 8b. Further, the capability of CA@CdS microbeads for detecting Hg^{2+} ions in the concentration range between 0.005 mg L^{-1} and 0.1 mg L^{-1} was demonstrated by using higher volumes of the Hg^{2+} ions. For example, the batch treated with 250 mL Hg^{2+} ions exhibited linear fluorescence quenching in the range of 0.025 and 0.10 mg L^{-1} (R^2 = 0.99, Fig. 8c), while the batch treated and 1500 mL Hg^{2+} ion solution exhibited linear fluorescence quenching in the range 0.015 and 0.035 mg/L (R^2 = 0.94,

Fig. 8d). Notably, the fluorescence quenching for CA@CdS microbeads treated with 0.005 mg L^{-1} Hg^{2+} ions was non-responsive as it was below the LOD.

3.4. Cation and anion interferences

The results of fluorescence quenching (I_o/I) of CA@CdS microbeads treated with 1 mg/L of Hg^{2+} ions in presence of batches of 10 mg/L of interfering cations, e.g., Na^+, K^+, Mg^{2+}, Ca^{2+}, Fe^{2+}, Mn^{2+}, Pb^{2+}, Cu^{2+}, As^{3+}, Cr^{3+}, Zn^{2+}, Cd^{2+} and Co^{2+}, respectively for optimized 30 min condition are shown in Fig. 9a. Notably, the I_o/I values were in the range between 2.0 and 2.5, which were significantly higher than those of the microbeads treated with the interfering cations (I_o/I = 1.02 to 1.24), except for Cu^{2+} (I_o/I =1.52). Our results are better than or comparable with cationic interference studies reported for cerium phosphonate nanoprobe,[42] CdTe quantum dots,[43] CdS QDs,[44] for Hg^{2+} detection. The selectivity for Hg^{2+} ion towards fluorescence quenching of CdS@CA over other metal ions can be attributed to relatively greater affinity of Hg^{2+} ions with sulphur.[45]

Further, the results of fluorescence quenching of CA@CdS microbeads treated with 1 mg L^{-1} of Hg^{2+} ions in presence of 1 mM of interfering anions, e.g., CH_3COO^-, Cl^-, CO_3^{2-}, HCO_3^-, HPO_4^-, OH^-, SeO_4^- SO_4^{2-} and BH_4^-, respectively are shown in Fig. 9b. Except for BH_4^-, the I_o/I values were 2-3 folds higher than the batches treated with only respective interfering anions. The application of CA@CdS microbeads was studied for real time Hg^{2+} ion sensing by spiking 1 mg/L and 0.5 mg/L of Hg^{2+} ions, respectively in batches of 50 mL test solution comprising of tap water conditioned to pH 6. The fluorescence quenching results of the test solution was compared with control batch of tap water which was not spiked with Hg^{2+} ion (Fig. 9c). Notably, the I_o/I value was determined as 2.28 (for 1 mg/L spike) and 1.71 (for 0.5 mg/L spike). Contrastingly, the I_o/I value for the control batch was determined as 1.0009, which is attributed to the absence of Hg^{2+}. Furthermore, ICP-MS analysis of the tap water used in this study confirmed Hg^{2+} ion

concentration to be less than the limit of detection, i.e., 0.002 mg/L. Therefore the observed fluorescence quenching in the test solutions that led to increase in the I_o/I values corresponded to the spiked Hg^{2+} ion concentration.

Ideally, batches of 0.5 mg/L and 1 mg/L of Hg^{2+} ions without interfering cations and anions should correspond to I_o/I values of 1.59 and 1.94 respectively. The deviation in the I_o/I value as a measure of Hg^{2+} concentration in real time spiked sample was 10-18 % higher. These higher I_o/I values can be accounted for enhanced fluorescence quenching by other cations and anions present in the tap water. In this regard, from Fig. 9a and 9b it may be commented that the interfering ions like Fe^{2+}, Cu^{2+}, Pb^{2+}, HCO_3^-, CO_3^{2-} which are commonly present in drinking water, are likely to contribute to the enhanced fluorescence quenching in the real time sample. It may therefore be concluded that the CA@CdS microbeads was an efficient mercury specific sensor and can be effectively used in analysing mercury levels in real time drinking water. Our results were comparable or better than other fluoroprobes and quantum dots reported as selective Hg^{2+} ion sensing.[46,47]

In order to determine minimum contact time required for detecting Hg^{2+} ions as compared to the interfering ions, the fluorescence quenching studies were conducted for 1 min, 2 min and 5 min contact time, respectively and the results are given in Fig. 9d-9f. Notably, the batch of 2 min contact time between Hg^{2+} ions with CA@CdS microbeads was optimum for measuring significant changes in fluorescence quenching for selectively detecting Hg^{2+} ions with respect to the interfering metal ions.

3.5. Mechanism of fluorescence quenching of CA@CdS and Hg^{2+} detection

From our studies, strong evidences were available regarding the effect of Hg^{2+} ion adsorption on CA@CdS microbeads and its consequential fluorescence quenching. First and the most striking result is the anomalous fluorescence quenching behaviour observed for the batch of

CA@CdS treated with Hg^{2+} ions (1 mg L^{-1}) in the presence of BH_4^- as interfering anions which did not reveal any fluorescence quenching, (Fig. 9b). The BH_4^- being a strong reducing agent, would reduce Hg^{2+} to elemental mercury, i.e. Hg(0). Unlike Hg^{2+}, Hg(0) would not interact with CA@CdS to cause any fluorescence quenching. This strongly suggested the need for Hg^{2+} ions for mercury detection by CA@CdS microbeads. Secondly, the phenomenon of adsorption of Hg^{2+} ion on CA@CdS microbeads is reflected from the plot of adsorption capacity (Q_t) measured at selected contact time (Fig. 10a). The adsorption capacity of CA@CdS microbeads for Hg^{2+} ions at equilibrium condition (achieved at 30 min contact time) was determined to be Q_e = 88.33 µg/g. The adsorption of Hg^{2+} was complemented with the large BET specific surface area (128.92 m^2/g) of the as-synthesized CdS QDs. Notably, the surface area of CdS QDs synthesized by us was significantly larger than reported in literature.[48] The equilibrium condition corresponding to adsorption phenomenon measured by ICP-MS analysis was similar to that of the fluorescence quenching study (shown in Fig. 3). Furthermore, the time dependent plot of fluorescence quenching (I_o/I) against adsorption capacity (Q_t) revealed a positive correlation (Fig. 10b), which strongly implied that the fluorescence quenching effect was due to adsorption of Hg^{2+} ions on CA@CDS microbeads.

The desorption study of Hg^{2+} ions from CA@CdS microbeads by various solvents e.g., water, 2 M HCl, 0.1 M HNO_3, 0.1 M EDTA, 0.1 M CH_3COONa and acidic thiourea (2 M HCl and 2% (w/v) thiourea), respectively provided useful insight about the possible interaction of Hg^{2+} with CA@CdS microbeads. Among these solvents, only acidic thiourea resulted in complete desorption of Hg^{2+} ions whereby ~ 99% fluorescence emission property of the CA@CdS microbeads was recovered, and the microbeads were successfully used for subsequent cycles for detection and removal of Hg^{2+} ions. A tentative model is presented here (Scheme 2) to explain an electrostatic interaction of Hg^{2+} ions with the lone pair of electrons on the sulphydryl group (i.e. CdS-S:). Our proposed model is in good agreement with the experimental evidences

where Hg^{2+} ions were successfully removed only when it was treated with acidic thiourea. The acidic condition was required for overcoming the non-bonded interaction between Hg^{2+} ions and the lone pair electrons of sulphydryl group, while thiourea was essential for restricting re-adsorption of Hg^{2+} on CA@CdS as the desorbed Hg^{2+} ions (a soft acid) have more affinity to bind with the sulphide ion (soft base) as suggested below :

$Hg^{2+} + SC(NH_2)_2 + H_2O \rightarrow HgS + OC(NH_2)_2 + 2H^+$

The desorbed Hg^{2+} ion has more affinity to form HgS owing to higher pK value as compared to that of Hg^{2+} ions adsorbed on CA@CdS via electrostatic interaction.

Next is to correlate the adsorption of Hg^{2+} ions with fluorescence quenching effect of CA@CdS microbeads. Firstly, it may be remarked that the fluorescence effect of CA@CdS was due to recombination of photoexcited electrons and holes of CdS QDs. The quenching effect in the fluorescence emission can be due to various reasons including inhibition of recombination of photoexcited electrons and holes. In the case of Hg^{2+} ions adsorbed in CA@CdS microbeads, it may be envisaged that the sulphydryl groups bound to CdS QDs bear a partially positive charge owing to their interaction with high electron affinity Hg^{2+} ions. Because of this, the photoexcited electrons are likely to be trapped at the sulphydryl group and trigger fluorescence quenching.

In the future, we would envisage improvement in the ability of using quantum dot based fluorescence probes immobilized in wider range of materials for detecting as well as separating contaminants. Further studies are required to assess the possibilities of detection different species of mercury and other analyte of interest. This method can be extended for biosensing applications as well.

4.0. Conclusions

A highly sensitive quantum dot based Hg^{2+} detection and scope for decontamination has been developed where mercaptoacetic acid stabilized CdS quantum dots were immobilized on calcium

alginate microbeads (CA@CdS microbeads). Though optimum condition for detection of mercury at concentrations less than 100 μg/L was 30 min but, qualitative detection of Hg^{2+} ions can be done in 2 min. The Hg^{2+} ion detection was based on fluorescence quenching, satisfying Stern-Volmer relationship. It has been comprehensively demonstrated that Hg^{2+} ions were adsorbed by interacting with the sulphydryl group of mercaptoacetic acid used for stabilizing CdS QDs which was key for fluorescence quenching by inhibiting recombination of photoexcited electron and holes. The other major advantage of this method is the ability of decontaminating Hg^{2+} owing to separation of Hg^{2+} ions adsorbed on microbeads by gravity. Overall, the results on Hg^{2+} detection at the levels of parts per billion are encouraging for developing a label-free fluoroprobe using CdS QDs immobilized on biocompatible substrate for sensing devices for environmental and biomedical applications.

Acknowledgement

Ambika Kumar is thankful to University Grants Commission (UGC), Government of India for granting Senior Research Fellowship (SRF). Authors are thankful to the Institute Instrumentation Centre of IIT Roorkee for electron microscopy studies.

References

1 K. P. Carter, A. M. Young and A. E. Palmer, *Chem. Rev.*, 2014, **114**, 4564–4601.

2 G.-H. Chen, W.-Y. Chen, Y.-C. Yen, C.-W. Wang, H.-T. Chang and C.-F. Chen, *Anal. Chem*., 2014, **86**, 6843-6849.

3 Y.-K. Yang, K.-J. Yook and J. J. Tae, *J. Am. Chem. Soc*., 2005**, 127 (48),** 16760-1676.

4 C.V. Hoang, M. Oyama, O. Saito, M. Aono and T. Nagao, *Sci. Rep.* 2013, **3** (**1175**) 1-6.

5 H. H. Harris, I. J. Pickering and G. N. George, *Science*, 2003, **301**, 1203.

6 B. C. Hopkins, J.D. Wilson and W.A. Hopkins, *Environ. Sci. Technol.*, 2013, **47**, 2416-2422.

7 L. Magos and T. W. Clarkson, Overview of the clinical toxicity of mercury, *Ann. Clin. Biochem*., 2006, **43**, 257–268.

8 J. L. Barringer, Z. Szabo and P. A. Reilly, *Current perspectives in contaminant hydrology and water resources sustainability*, ed. P.M. Bradley, InTech Publisher, ISBN 978-953-51-1046-0, 2013.

9 Q. Wang, Q. Wang, D. Kim, D. D. Dionysiou, G. A. Sorial and D. Timberlake, *Environ. Pollut.,* 2004, **131**, 323-336.

10 United States Environmental Protection Agency. Mercury Study Report to Congress, Vol V, Health effects of mercury and mercury compounds, EPA-452/R-97-007 December 1997, Available at: http://www.epa.gov/ttn/caaa/t3/reports/volume5.pdf

11 S. Gil, I. Lavilla and C. Bendicho, *Anal. Chem*., 2006, **78** 6260-6264.

12 D. Yan, L. Yang and Q. Wang, *Anal. Chem*., 2008, **80**, 6104-6109.

13 W. Meng, F. Weiyue, S. Junwen, Z. Fang, W.Bing, Z. Motao, L. Bai, Z. Yuliang and C. Zhifang, *Talanta*, 2007, **71**, 2034-2039.

14 E. M. Nolan and S. J. Lippard, *Chem. Rev.,* 2008, **108**, 3443–3480.

15 G. Chen, Z. Guo, G. Zeng, L. Tang, *Analyst*, 2015 DOI: 10.1039/c5an00389j.

16 P. Mahato, S. Saha, P. Das, H. Agarwalla and A. Das, *RSC Adv.,* 2014, **4**, 36140-36174

17 L. Basabe-Desmonts, D.N. Reinhoudt and M. Crego-Calama, *Chem. Soc. Rev*., 2007, **36**, 993-1017.

18 C. Xing, L. Liu, X. Zhang, H. Kuang and C. Xu, *Anal. Methods*, 2014, **6**, 6247- 6253.

19 Y. Zhu, D. Deng, L. Xu, Y. Zhu, L. Wang, B. Qi and C. Xu, *Food Agric. Immunol.,* 2015, **26 (4),** 512-520.

20 A. Singh, R. Pasricha and M. Sastry, *Analyst*, 2012, **137**, 3083-3090.

21 V. N. Mehta and S. K. Kailasa, *RSC Adv.,* 2015, **5,** 4245-4255.

22 W. Ma, M. Sun, L. Xu, L. Wang, H. Kuang and C. Xu, C*hem. Commun*., 2013, **49**, 4989-4991

23 L. Xu, H. Yin, W. Ma, H. Kuang, L. Wang and C. Xu, *Biosens. Bioelectron*., 2015, **67**, 472- 476.

24 C. Yuan, K. Zhang, Z. Zhang and S. Wang, *Anal. Chem.* 2012, **84 (22),** 9792-9801.

25 J. Ke, X. Li, Q. Zhao, Y. Hou and J. Chen, *Sci. Rep*., 2014, **4**, Article Number 5624, DOI:10.1038/srep05624.

26 N. B. Pendyala and K. S. R. K. Rao, *Colloid. Surf. A*., 2009, **339**, 43-47.

27 S. Xiangying, L. Bin and X. Yibang, *Analyst,* 2012, **137**, 1125-1129.

28 M. Koneswaran and R. Naranswamy, *Sensor. Actuat. B*., 2009, **139**, 91-96.

29 B. B. Campos, M. Algarra, B. Alonso, C.M. Casado and J.C.G. Esteves da Silva, *Analyst* 2009, **134**, 2447-2452.

30 B. P. Nenavathu and R. K. Dutta, *Adv. Mat. Lett*., 2013, **4**, 359-362.

31 R. Bannerjee, R. Jayakrishnan and P. Ayyub, *J. Phys.: Condens. Matter.,* 2000, **12,** 10647–10654.

32 A. P. Alivisatos, *Science*, 1996, **271 (5251)**, 933-937.

33 W. Chansuvarn, T. Tuntulani and A. Imyim, *Trend. Anal. Chem.,* 2015, **65**, 83-96

34 Z. Fang, Y. Wang, J. Song, Y. Sun, J. Zhou, R. Xu and H. Duan, *Nanoscale*, 2013, **5**, 9830–9838.

35 D. Sarkar, C. K. Ghosh and K. K. Chattopadhyay, *CrystEngComm*, 2012, **14**, 2683-90.

36 F. Xu, Y. Yuan, H. Han, D. Wu, Z. Gao and K. Jiang, *CrystEngComm,* 2012, **14**, 3615-3622.

37 L. E. Brus, *J. Chem. Phys*. 1984, **80 (9)**, 4403-4409.

38 I. Tamiolakis, I. N. Lykakis, A. P. Katsoulidis and G. S. Armatas, C*hem. Commun*., 2012, **48**, 6687-6689.

39 Y.-L. Lee and Y.-S. Lo, *Adv. Funct. Mater.,* 2009, **19**, 604-609.

40 C. Madhu, A. Sundaresan and C. N. R. Rao, *Phys. Rev. B*., 2008, **77**, 201306(R).

41 E. G. Janzen, *Acc. Chem. Res.,* 1971, **4**, 31-40.

42 Y. P. Zhu, T.-Y. Ma, T.-Z. Ren and Z.-Y. Yuan, *ACS Appl. Mater. Interfaces,* 2014, **6 (18)**, 16344-1635.

43 J. Pei, H. Zhu, X. *W*ang, H. Zhang and X. Yang, *Anal. Chim. Acta.* 2012, **757**, 63-68.

44 M. Koneswaran and R. Narayanswamy, *Microchim. Acta*., 2012, **178**, 171-178.

45 H. Son, J. H. Lee, Y-R. Kim, I. S. Lee, S. Han, X. Liu, J. Jawarsky and J. H. Jung, *Analyst*. 2012, **137**, 3914-3916.

46 Y. Lou, Y. Zhou, J. Chen and J.-J. Zhu, J. *Mater. Chem. C*, 2014, **2**, 595-613.

47 D. Liu, W. Qu, W. Chen, W. Zhang, Z. Wang and X. Jiang, *Anal. Chem.,* 2010, ***82*** **(23)**, 9606–9610

48 J.-W. Shi, Z. Wang, C. He, H. Wang, J.-W. Chen, M.-L. Fu, G. Li and C. Nilu, *J. Mol. Catal. A: Chem.,* 2015, **399**, 79–85.

FIGURE CAPTION

Fig. 1. UV-visible absorption (dashed black) and fluorescence emission (solid blue) spectra of MAA capped CdS QDs. **(a)** The band gap of MAA capped CdS QDs was determined to be 380 nm and the **(b)** corresponding maximum fluorescence emission (solid blue) is determined at λ_{em} = 534 nm, using λ_{ex} = 375 nm.

Fig. 2. Fluorescence quenching study of CA@CdS microbeads with different pH of Hg^{2+} ions, ranging from pH = 3 to pH = 7

Fig. 3. Time dependent fluorescence quenching study of CA@CdS microbeads treated with 1 mg/L of Hg^{2+} ion concentration over a time period ranging between 1 min and 90 min

Fig. 4. X-ray diffraction (XRD) pattern of as synthesized CdS quantum dots

Fig. 5. (a) Transmission electron microscopy (TEM) image of as synthesized CdS quantum dots (inset: fitting of a histogram showing size distribution of CdS QDs);
(b) high resolution TEM (HRTEM) of CdS QDs revealing lattice fringes as marked by the arrows and inset represents selected area electron diffraction (SAED) pattern of CdS QDs

Fig. 6. SEM images of CA@CdS microbeads (a) showing irregular spherical shapes of microbeads (b) showing morphological features at 200x magnification, (c) showing nanoparticles at the surface of the microbeads recorded at 10000x magnification, (d) EDX spectrum of CA@CdS microbeads, revealed characteristic X-ray peaks of Cd and S indicating presence of CdS QDs at the surface of microbeads (e) Line scanning FE-SEM image of surface and cross sectional part of CA@CdS microbeads, showing CdS QDs are present only at the surface of microbeads

Fig. 7. FT-IR spectrum of (a) CA@CdS microbeads and (b) Mercaptoacetic acid (MAA)

Fig. 8. (a) Showing reduction in the intensity of the fluorescence emission of CA@CdS microbeads treated with increasing concentration of Hg^{2+} ions; (b) linear Stern-Volmer plot in the Hg^{2+} ion concentration range of 0.1 mg/L to 2.0 mg/L; (c) linear Stern-Volmer plot for Hg^{2+}

ions concentrations ranging from 0.025 mg/L to 0.100 mg/L, where the analyte volume = 250 mL; (d) showing linear Stern-Volmer plot for Hg^{2+} ions concentrations ranging from 0.005 mg/L to 0.035 mg/L, where analyte volume = 1500 mL

Fig. 9. Showing selectivity of fluorescence quenching effect of CA@CdS microbeads treated with Hg^{2+} ions in presence of interfering (a) metal cations; (b) anions; (c) plot showing detection of Hg^{2+} in a spiked tap water sample; (d) fluorescence quenching study of CA@CdS microbeads treated with 1 mg/L Hg^{2+} in presence of different interfering metal ions, at contact time, 1 min, (e) contact time = 2 min and (f) contact time = 5 min

Fig. 10 (a) Kinetic studies on adsorption of the Hg^{2+} ion on the CA@CdS microbeads, analysed by ICP-MS. Here, $Q_t = [(C_0 – C_t)*V]/m$; where C_o is the initial concentration of Hg^{2+} ions, C_t = Concentration of Hg^{2+} ions in the supernatant after time t, V = volume of the Hg^{2+} ion used in the study, m = mass of the adsorbent, i.e., CA@CdS microbeads;

(b) Plot showing fluorescence quenching (I_0/I) verses adsorption capacity (Q_t) of Hg^{2+} ions by CA@CdS microbeads at time intervals ranging between 2 min and 90 min

Scheme 1. A representative schematic diagram showing anchoring of CdS QDs with calcium alginate matrix through different terminal functional groups of mercaptoacetic acid as capping agent

Scheme 2. Schematic diagram showing interaction of Hg^{2+} ions with CA@CdS microbeads, resulting in decrease in fluorescence intensity of microbeads

FIGURES

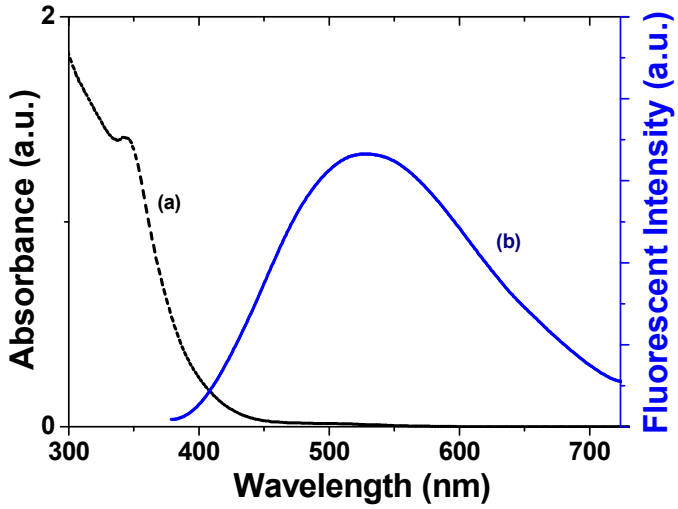

Fig. 1

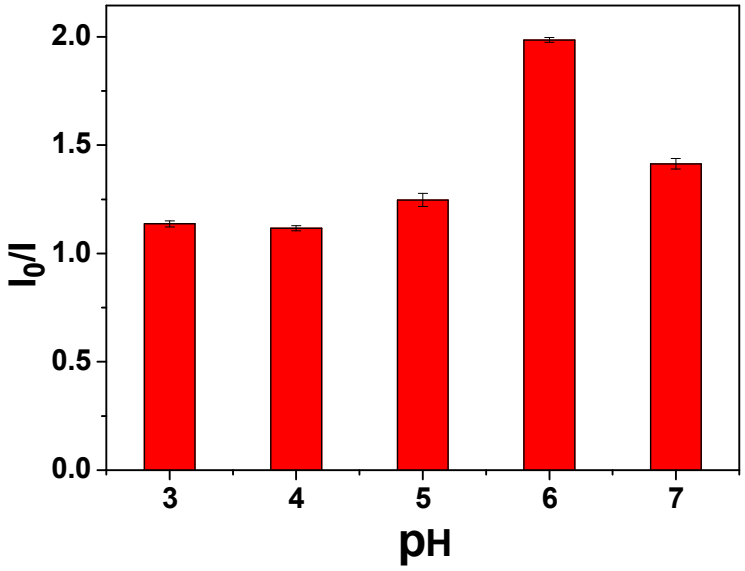

Fig. 2.

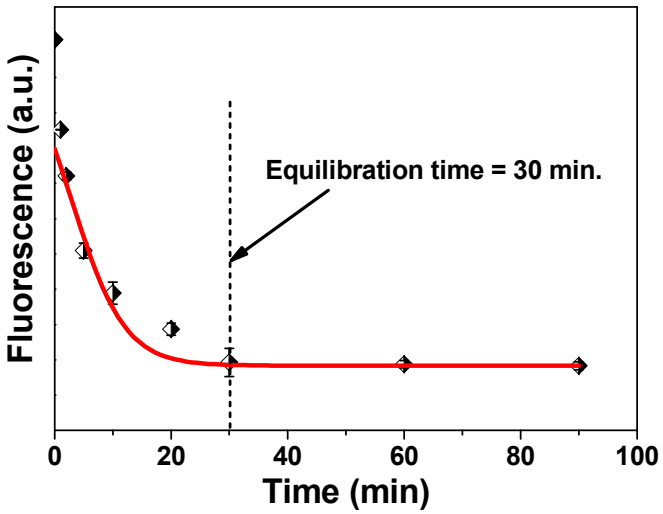

Fig. 3.

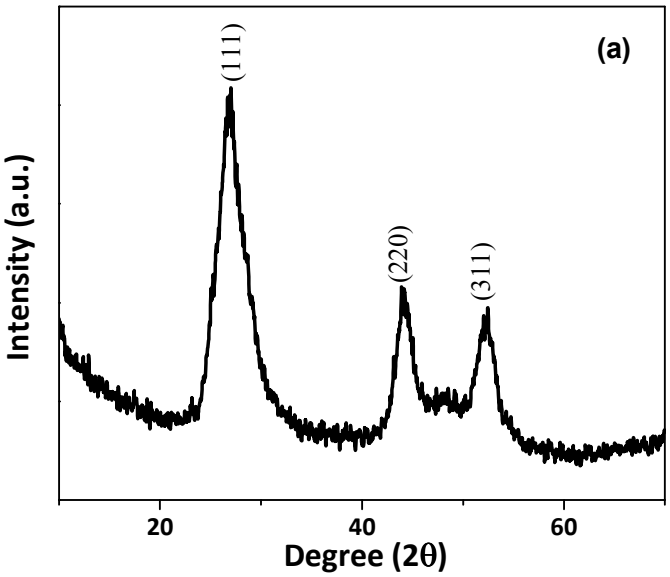

Fig. 4.

(a)

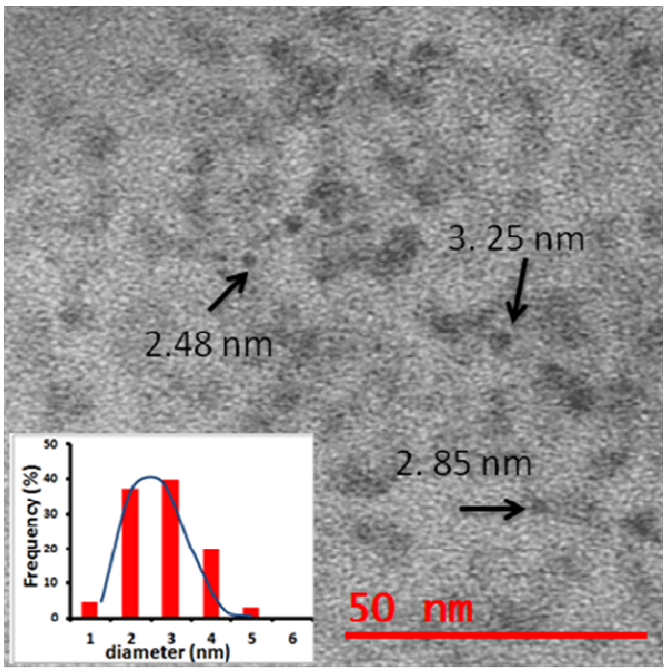

(b)

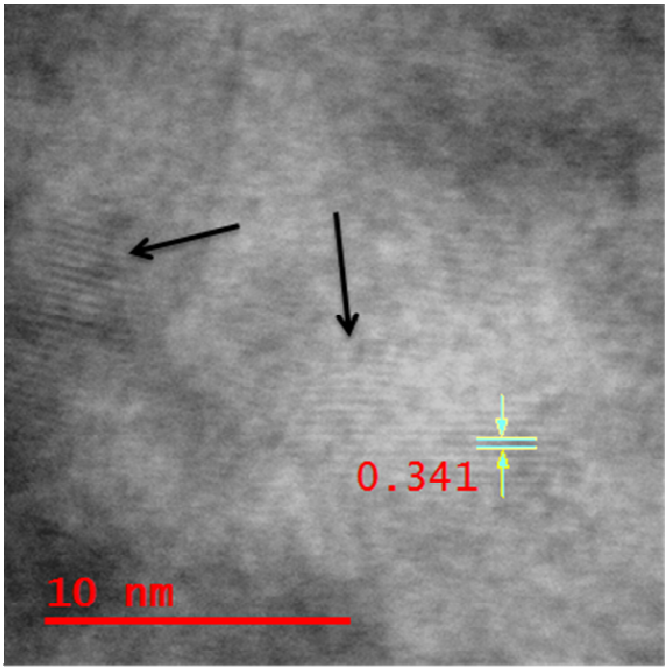

Fig. 5.

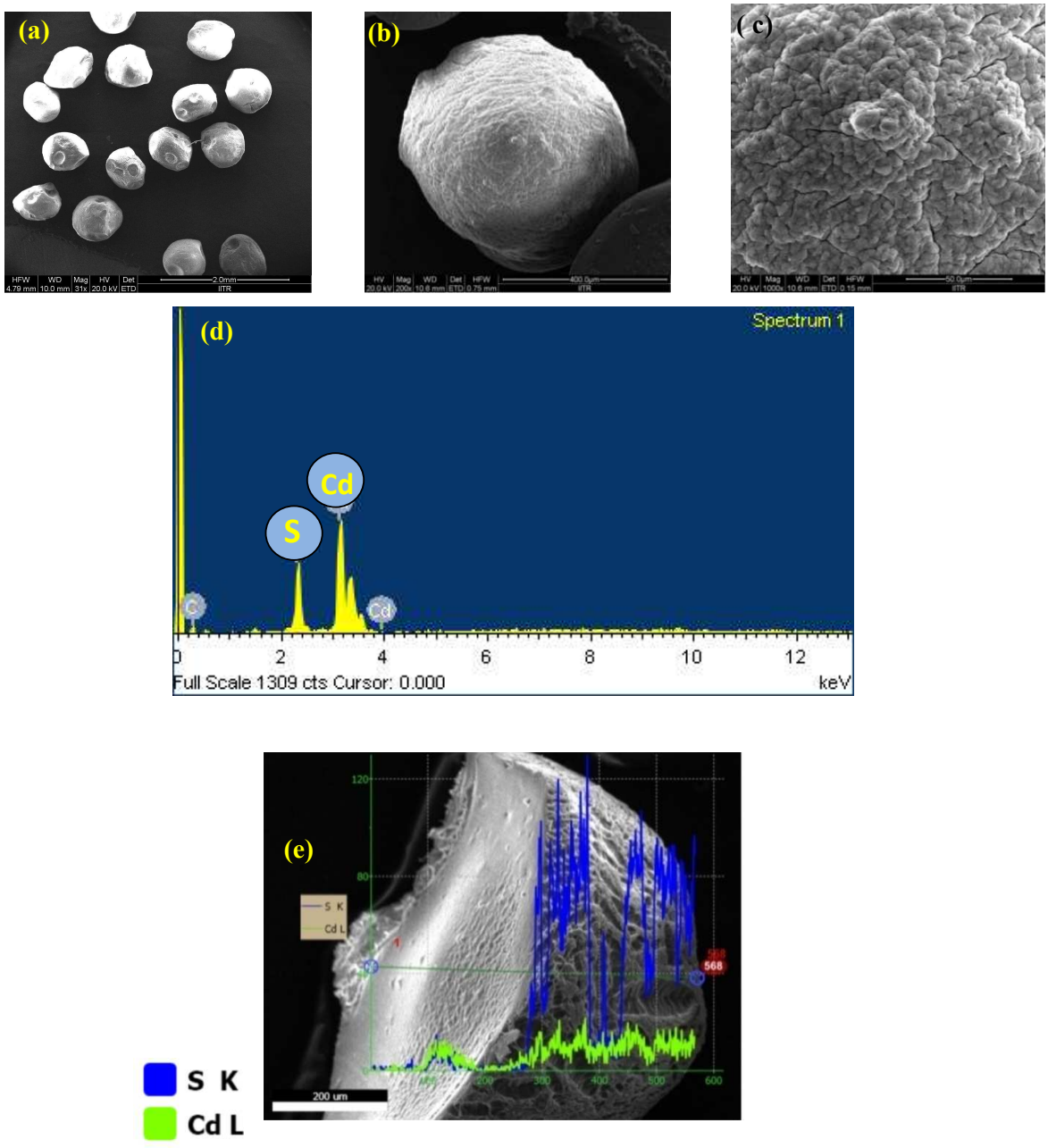

Fig. 6.

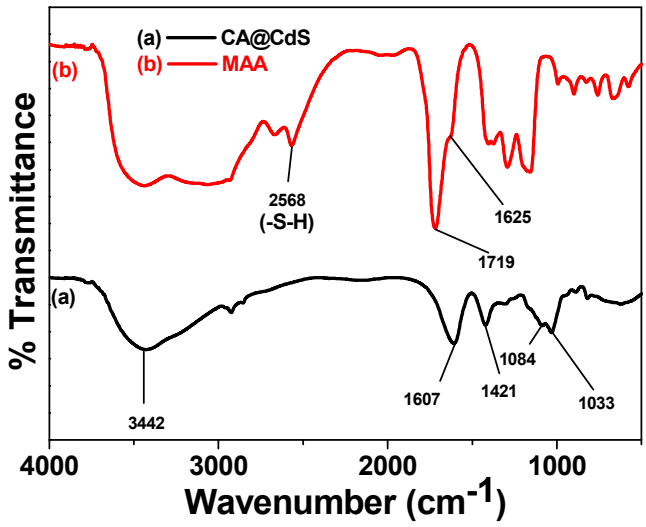

Fig. 7.

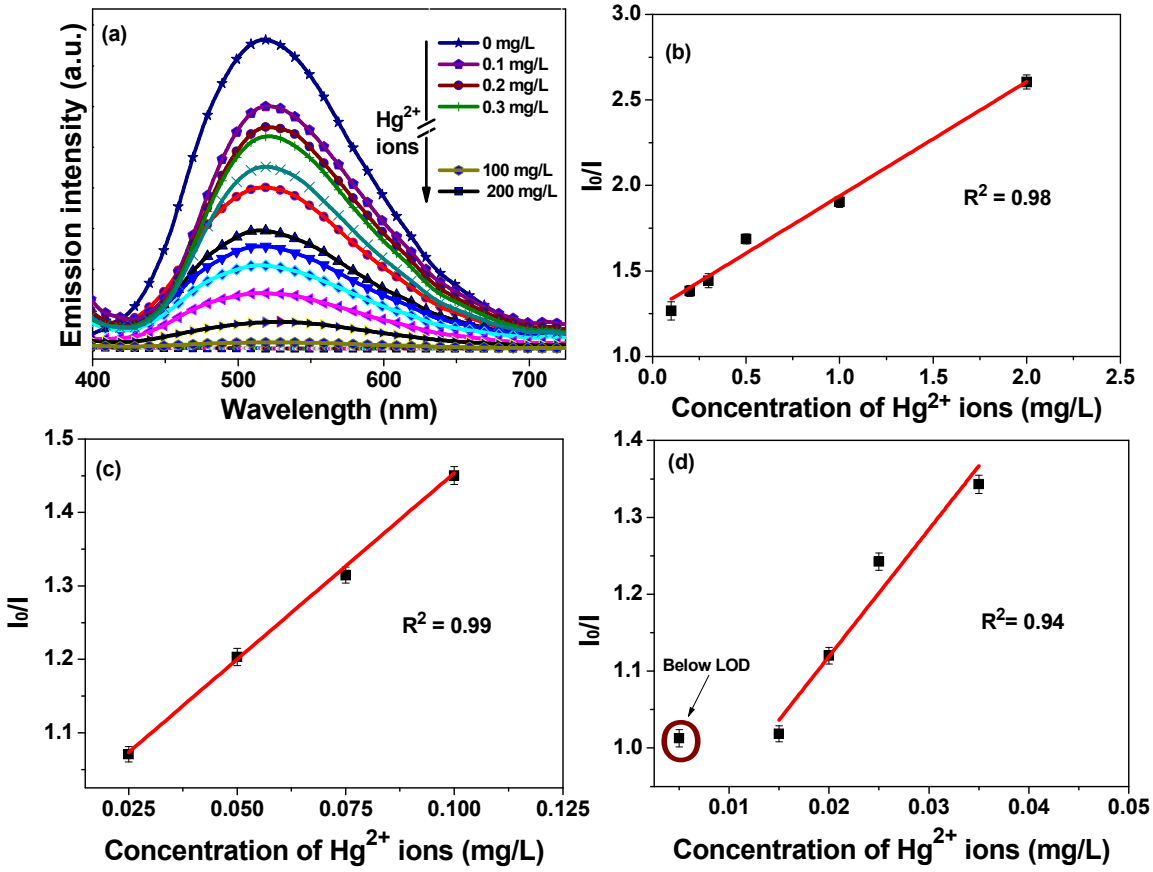

Fig. 8.

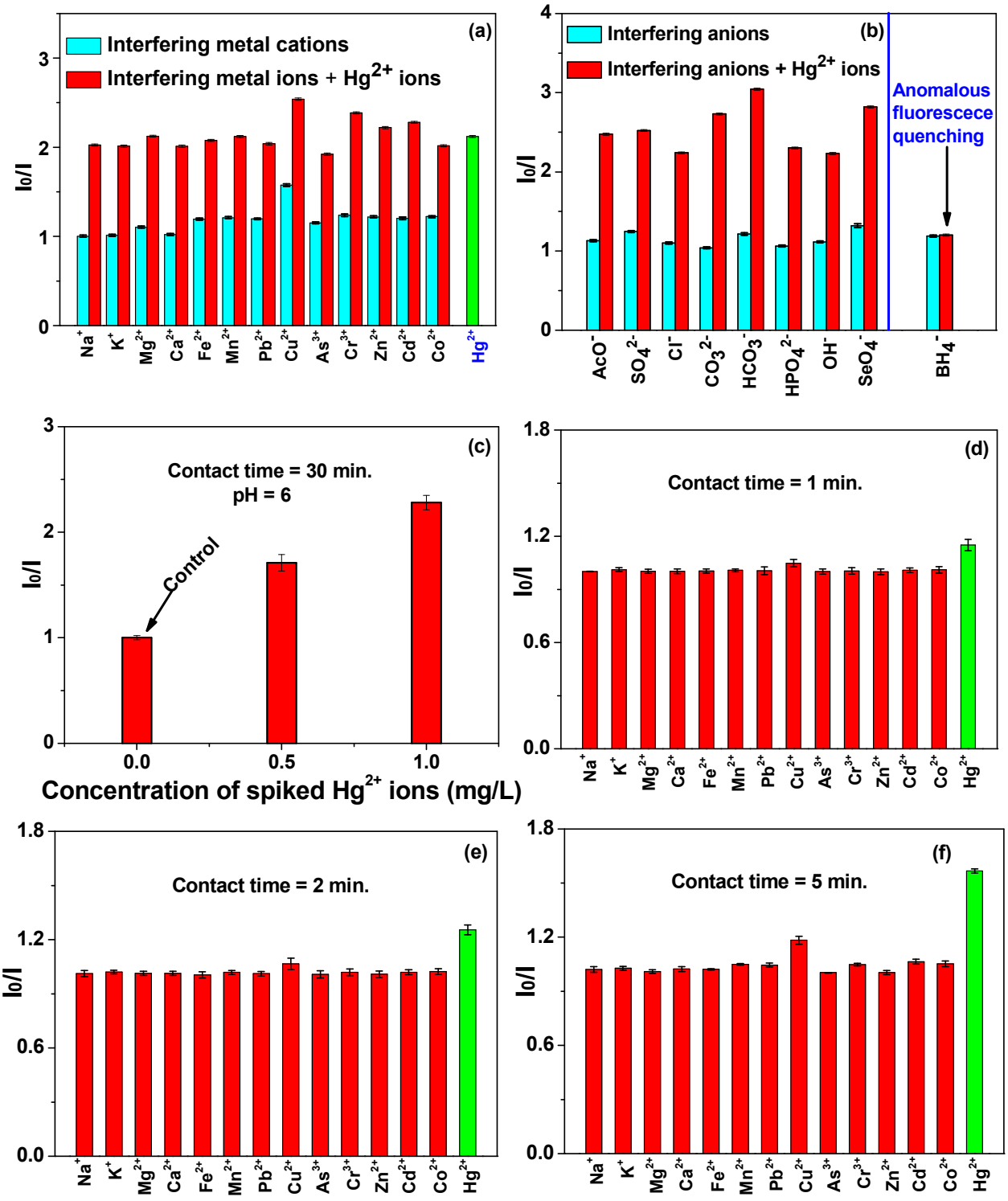

Fig. 9.

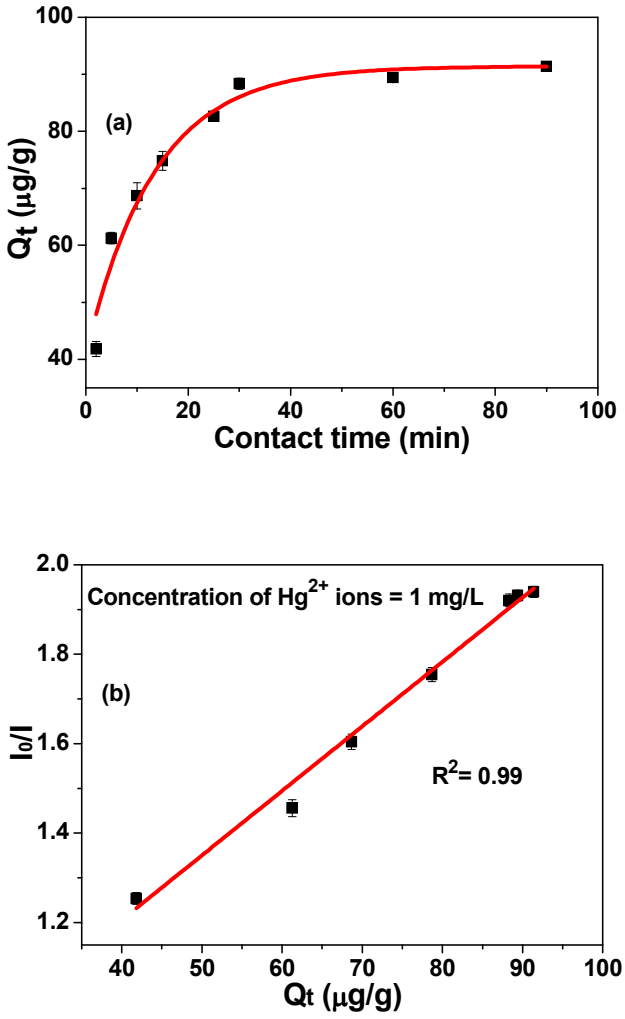

Fig. 10.

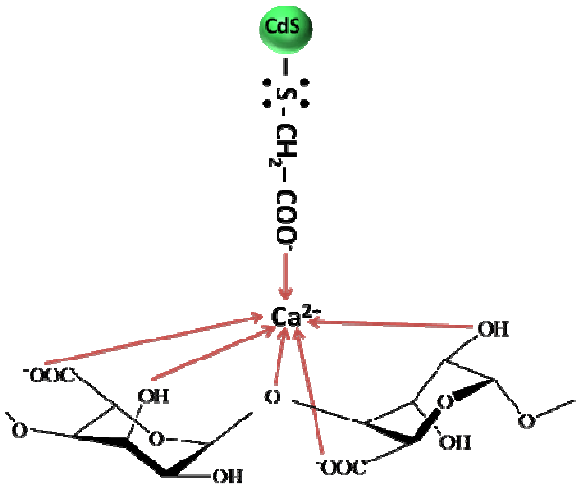

Scheme 1.

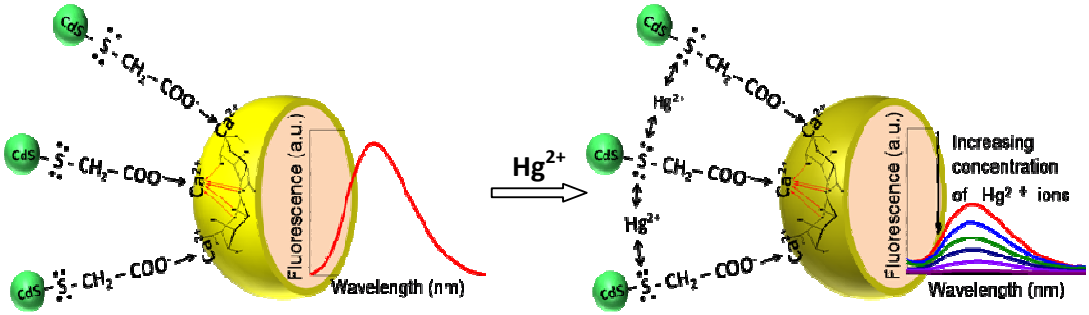

Scheme 2.